Response to Reviewer Comments

We thank the reviewer for the constructive comments and suggestions, which helped us improve the clarity and quality of the manuscript. In this response letter, we provide point-by-point responses. Our replies to the reviewers' comments are presented **in blue font**, while the corresponding revisions in the manuscript are indicated **in blue italics with yellow highlights**, together with the **updated line numbers**.

Comment:

1. The star marker in Figure 1 is missing. Please ensure that all markers mentioned in the text are present in the figure.

We appreciate the reviewer for pointing this out. We have added the missing star marker in Figure 1a to indicate the starting locations of the aircraft measurements, as described in the figure caption. We also carefully checked all other figures to ensure that no additional markers are missing.

L 120:

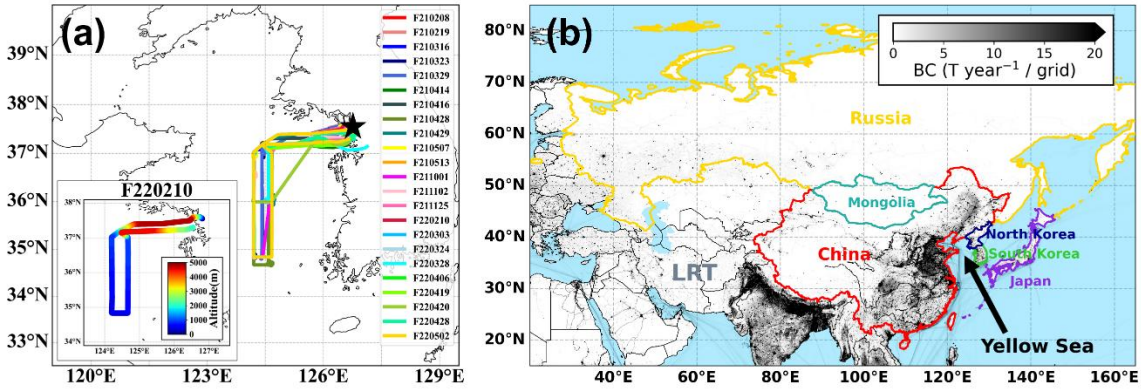

Figure 1. (a) Flight paths for all 23 research flights conducted in this study. All flights departed from the location marked with a star. Different colors represent individual flights. The bottom-left panel shows the flight track for F220210, color-coded by altitude as a representative example of the vertical flight profiles. (b) Black carbon emission rates (tons per year / 0.1° × 0.1° grid cell) with regions where air masses influencing the observations during the aircraft mission (South Korea, North Korea, Japan, China, Mongolia, Russia, and LRT in different colors). BC emissions are sourced and averaged from EDGARv8.1 (Crippa et al., 2024) data for 2021 and 2022.

2. Line 62: A recent study (Hu et al., EST Letters, 2022, 10.1021/acs.estlett.2c00060) identified the fraction of more spherical BC which can support your statements about the influence of particle morphology on BC absorption properties.

Thank you for this valuable suggestion. We have incorporated the reference and expanded the discussion accordingly:

L 58–61:

"Recently, Hu et al. (2022) reported that freshly emitted or only slightly coated BC generally exhibits a fractal-like structure, becoming progressively more spherical as coatings fully envelop the core. This gradual change toward sphericity is closely linked to the efficiency of the lensing effect that enhances BC light absorption."

3. Line 89: The aircraft measurements about BC over China were also conducted in recent studies (Hu et al, Chemosphere, 2020, 1016/j.chemosphere.2020.126455; Tian et al., ACP, 2020, 10.5194/acp-20-2603-2020; Liu et al., ERL, 2019, 10.1088/1748-9326/ab4872) could be cited to discuss aircraft measurement experiments conducted over the Chinese megacities of Beijing and Xuzhou.

We agree with the reviewer's suggestion and have added these references both in the Introduction and in the Results and Discussion sections:

L 93–95:

"Most recent aircraft studies over Asia have focused on observations conducted primarily over inland urban areas including Chinese megacities such as Beijing and Xuzhou (Hu et al., 2020; Liu et al., 2019a; Tian et al., 2020), with limited coverage of marine or downwind regions."

L 366–369:

"Similar aloft-enhanced processes were also reported by Liu et al. (2019a), reported enhanced secondary aerosol formation and BC coating above the PBL under strong midday solar radiation, emphasizing the role of upper-atmosphere photochemistry in driving BC aging under intense sunlight."

4. Line193-195: Please provide a justification for choosing a height of 2.5 km instead of other

heights.

Since BC is emitted near the surface, our aircraft observations show that rBC mass concentrations sharply decline above ~3 km, likely suggesting that vertical mixing processes can effectively loft surface-emitted BC to altitudes approaching 3 km before significant dilution or removal occurs.

To focus on the lower troposphere where surface emissions remain influential, we selected 2.5 km as a conservative upper bound for analysis. This threshold is supported by previous studies indicating that land-based PBLH can reach up to ~2 km under favorable convective conditions (Gu et al., 2020; Qu et al., 2017). Furthermore, several regional aerosol transport studies have adopted 2.5 km as a practical reference altitude (Kanaya et al., 2013; Kanaya et al., 2016; Choi et al., 2020), while Lamb et al. (2018) used model-derived mixing depths along trajectories for similar purposes.

The manuscript text has been revised accordingly to incorporate this clarification.

L 202–205:

"Following previous studies (Choi et al., 2020b; Kanaya et al., 2013, 2016), the country most frequently traversed by each trajectory below 2.5 km altitude was designated as the origin of the air mass. This threshold reflects the fact that, under favorable convective conditions, the PBL over land can extend up to ~2 km (Gu et al., 2020; Qu et al., 2017), allowing surface-emitted aerosols to reach at least this altitude."

5. Line 187: Clarify whether the 10s indicates outputting one trajectory every 10 seconds or if it represents the time step for one trajectory. If it is the output frequency, explain how it is implemented. If it is the time step, note that the minimum time step in HYSPLIT is 1 minute, as mentioned in the HYSPLIT Limitations. Additionally, provide information about your target site.

The '10s' refers to the interval of our observational data, not to the HYSPLIT model time step. For each 10 seconds observation along aircraft flight tract (latitude, longitude, and altitude), we computed a back trajectory using HYSPLIT model. Because HYSPLIT requires meteorological input at hourly resolution, the 10 seconds observation times were rounded to the nearest hour

when they supplied to the model. We have revised the manuscript to clarify this point.

The information on our target site, Yellow Sea is written as follows.

L 116–118:

"The YS, located west of the Korean Peninsula and downwind of continental East Asia, serves as an ideal receptor site for observing air masses transported from continental regions toward the Korean Peninsula under the prevailing westerlies."

In our HYSPLIT modeling, backward air mass trajectories were calculated at each observational point over the Yellow Sea, it is clearly indicated in the following sentence.

L 195–197:

"At 10-second intervals along the flight track over the YS, 5-day back trajectories were computed using the Global Data Assimilation System (GDAS1, 1 ° × 1 ° resolution), consistent with BC's atmospheric lifetime. "

6. The different types of pollution in Figure 2 are interesting. However, the authors did not conduct further analysis and research on this. Please explain the reason for classifying pollution types and how it contributes to the study's objectives.

Earlier versions of the manuscript included more detailed analysis of haze and dust events; these were later streamlined to focus on the main objectives. Nevertheless, we retained the indication of pollution events in Figure 2 because our multi-year aircraft measurements inevitably sampled a variety of atmospheric conditions. Marking Asian Dust and Haze episodes helps readers interpret day-to-day variations in concentration and mixing state and provides useful context for other researchers interested in these events over the Yellow Sea. We have added corresponding content to the manuscript.

L 271–274:

"In addition, we captured several episodic events including "Haze", "Asian Dust", and the mixed "Haze & Asian Dust", as classified by Korea Meteorological Administration (KMA). During Asian Dust episodes, most variables remained comparable to the other days, except for a noticeable decrease in BC's internal mixing. In contrast, Haze events were characterized by substantial

increases in the average values of all observed parameters. Thus, both size distributions (MMD) and mixing state (F_{thick} and $R_{shell/core}$) of rBC particles observed in this study clearly indicate their considerable dependence on the origins and further chemical/physical processes of the air masses during transport to this remote environment."

7. Figure 4: The figure suggests a regional transmission process above 3000 m in autumn, leading to changes in BC mass and MMD. However, this result is not reflected in the coating thickness, which appears to maintain the same trend as at low altitudes. Please provide an explanation for this observation.

We appreciate this insightful comment. For more detailed analysis and discussion, we have added two figures in SI (Figure S7 and Figure S8).

Prior to discussing the autumn observations in detail, we briefly address the complexity of rBC mixing state characteristics identified in our measurements. Our data analysis demonstrates the observed BC's internal mixing over the Yellow Sea is primarily determined by the source origin of air masses. Table 2 summarizes the average rBC properties by major source region ('Major Region') identified using backward air mass trajectories. The majority of air masses originated from China (62 %), which exhibited the high degree of rBC internal mixing, whereas those classified as Long-Range Transport (LRT) showing the lowest. This airmass origin-varying physical properties of rBC particles influenced their vertical profiles (Figure 4). In winter, Chinese air masses dominated below 2.5 km (74 %), whereas above this altitude, the LRT contribution rises to 88 % (Figure S7), accompanied by sharp decreases in both F_{thick} and $R_{shell/core}$ (Figure 4). In contrast, during spring, together with potentially enhanced photochemical reaction at upper altitude, the contrast in source regions was less pronounced, leading to more moderate vertical gradients in mixing-state parameters.

Regarding the autumn observations, figure S7 shows the vertical profiles of rBC properties and accumulated precipitation along trajectories (APT) for each daily observation during the autumn. The autumn campaign included three aircraft flight days. Among them, two flights (F211001 and F211102) exhibited very similar vertical profiles of rBC properties and APT. Meanwhile, during F211125, a sharp decrease in M_{rBC} and MMD was observed above ~2 km, coinciding with an increase in APT to ~2–6 mm. This alignment suggests that rBC particles, particularly larger ones, were scavenged by precipitation, leading to the observed reductions in M_{rBC} and MMD. This

episodic case (F211125) influenced the average shape of the autumn vertical profile (Figure 4).

However, two mixing-state parameters (F_{thick} and $R_{shell/core}$) did not follow the same vertical patterns as M_{rBC} and MMD. Compared to the other seasons, both F_{thick} and $R_{shell/core}$ remained consistently high with altitude on all three autumn flight days, likely due to the combined effects of (i) enhanced photochemical production of coating materials and shorter transport distance than winter and (ii) the relatively low solubility of those coatings, etc. Meanwhile, the vertical gradient of $R_{shell/core}$ was steeper than that of F_{thick}. This can be attributed largely to their size-selection difference in methods: F_{thick} is determined from all detected rBC particles (~70–510 nm), whereas $R_{shell/core}$ is derived from rBC cores in the 140–220 nm range. Preferential wet scavenging of larger rBC core (and/or soluble coating) at upper altitude likely contributed to the steeper decline of $R_{shell/core}$ with altitude at some extent.

These findings demonstrate that the rBC mixing state is primarily determined by combustion activity and conditions at the source, but is further modified significantly by atmospheric processes such as wet scavenging and photochemical reaction, ultimately shaping its seasonal vertical structure. These discussions have been added as follows.

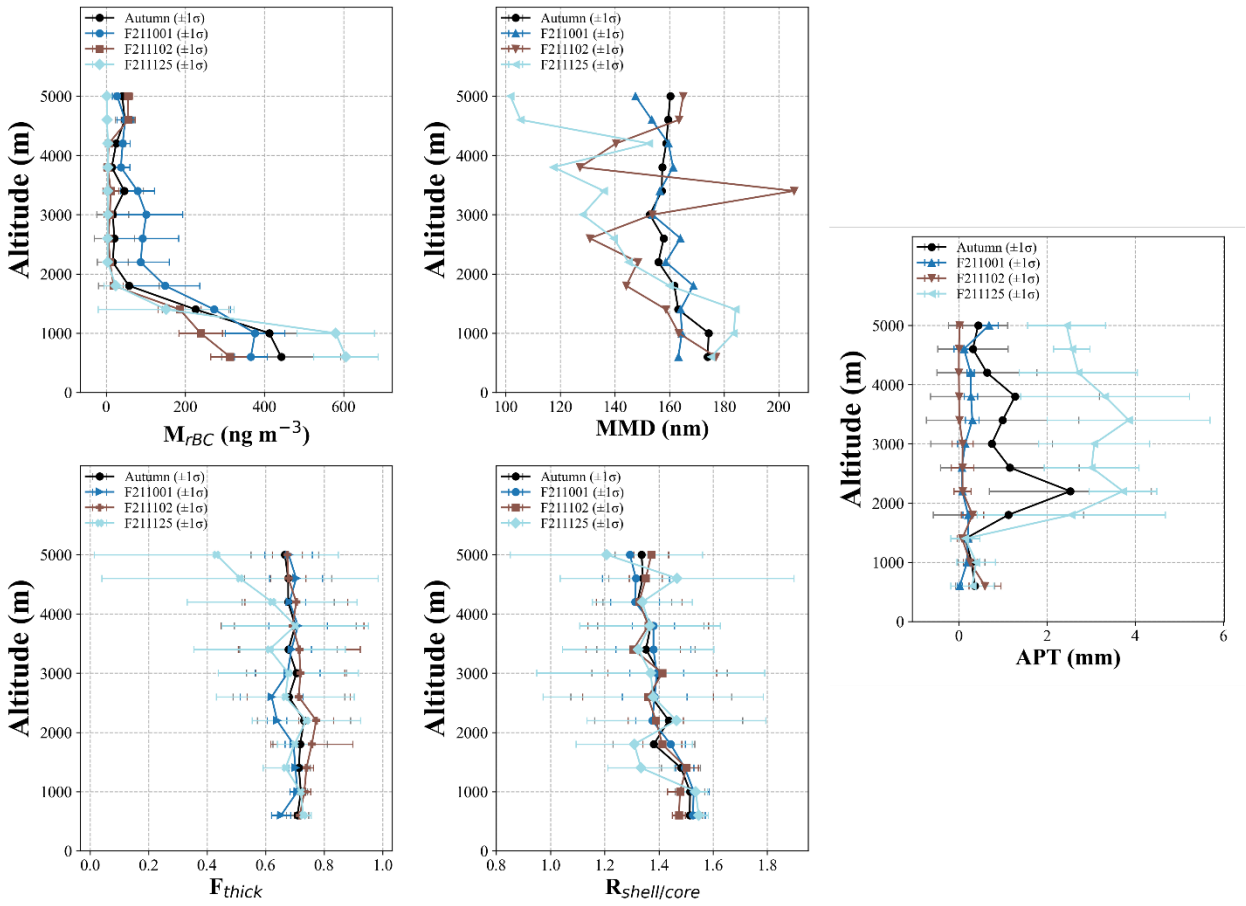

Figure S7. Vertical profiles of rBC particles (M_{rBC}, MMD, F_{thick}, $R_{shell/core}$, APT) for 2021 Autumn (Oct.–Nov.), F211001, F211102 and F211125. Horizontal error bars indicate ± 1 σ (standard deviation) variability within each altitude bin.

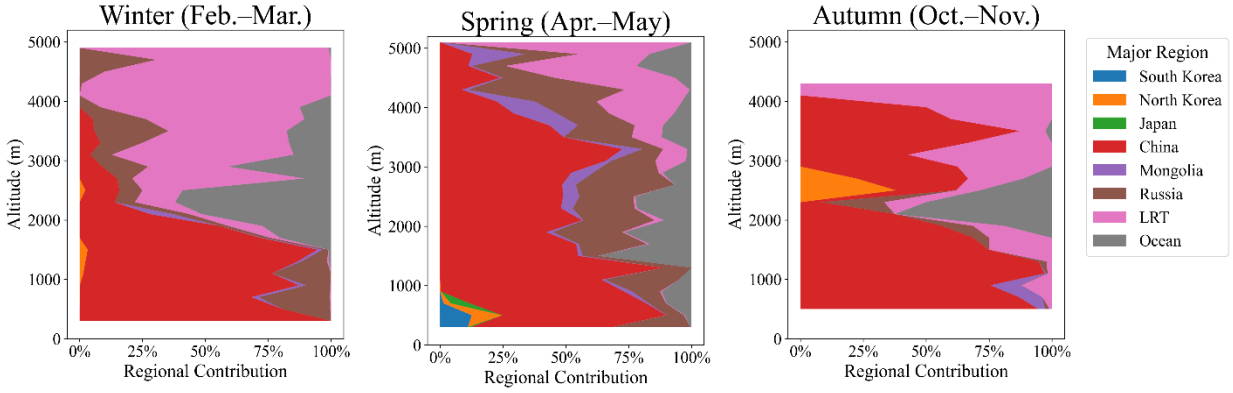

Figure S8. Seasonally varying vertical contributions of Major Regions for Winter, Spring, and Autumn.

L 344–359:

"In line with these studies, our findings suggest that aged rBC particles transported to high altitudes (above ~3 km) undergo significant physical transformation largely due to wet scavenging processes such as precipitation and cloud interaction, highlighting the strong sensitivity of both their size and mixing state to these removal mechanisms.

As a case, during F211125 in the autumn, a sharp decrease in M_{rBC} and MMD was observed above ~2 km, coinciding with an increase in APT to ~2–6 mm (Figure S7). This alignment suggests that rBC particles, particularly larger ones, were scavenged by precipitation, leading to the observed reductions in M_{rBC} and MMD. This episodic case (F211125) influenced the average shape of the autumn vertical profile (Figure 4). However, two mixing-state parameters (F_{thick} and $R_{shell/core}$) did not follow the same vertical patterns as M_{rBC} and MMD. Compared to the other seasons, both F_{thick} and $R_{shell/core}$ remained consistently high with altitude on all three autumn flight days (Figure S7), likely due to the combined effects of (i) enhanced photochemical production of coating materials and shorter transport distance than winter and (ii) the relatively low solubility of those coatings, etc. Meanwhile, the vertical gradient of $R_{shell/core}$ was steeper than that of F_{thick}. This can be attributed to their size-selection difference in methods: F_{thick} is determined from all detected rBC particles (~70–510 nm), whereas $R_{shell/core}$ is derived from rBC cores in the 140–220 nm range. Preferential wet scavenging of larger particles at upper altitude likely contributed to the steeper decline of $R_{shell/core}$ with altitude at some extent. "

L 427–434

"This airmass origin-varying physical properties of rBC particles influenced their vertical profiles (Figure 4). In winter, Chinese air masses dominated below 2.5 km (74 %), whereas above this altitude, the LRT contribution rises to 88 % (Figure S7), accompanied by sharp decreases in both F_{thick} and $R_{shell/core}$ (Figure 4). In contrast, during spring, together with potentially enhanced photochemical reaction at upper altitude, the contrast in source regions was less pronounced, leading to more moderate vertical gradients in mixing-state parameters. These findings provide clear evidence that the vertical structure of rBC mixing state is fundamentally shaped by combustion characteristics at the source region and thus vary seasonally with changes in air mass origin. This structure is further modified by atmospheric processes such as wet scavenging and photochemical aging.

L504 in Conclusion:

"Our observational results from YS provide the clear evidence that the vertical structure of rBC's mixing state was fundamentally shaped by combustion characteristics at the source region and further modified substantially by atmospheric processes such as wet scavenging and photochemical aging."

8. Figure 5a: The transport processes of gases and aerosols differ below and above the boundary layer. Explain how the authors justify using the same fitting result to represent the results at different heights. Additionally, discuss the reason for Russia's significantly lower r2 compared to other regions.

We acknowledge that transport processes differ between the planetary boundary layer (PBL) and the free troposphere (FT).

In an earlier version of the analysis, we applied separate fits for data within the PBL and in the FT, but except for a few cases such as Russia, the slopes and correlations were nearly identical to those obtained with a single fit. As shown in Figure 5a, the data points from the PBL and FT are distinguished by different markers, yet the relationship between M_{rBC} and CO is well described by essentially the same slope, which justified using a single fitting line to represent both altitude ranges.

Regarding the relatively low R^2 for Russia (0.34), several factors may contribute:

- Source heterogeneity: High R^2 values primarily imply that M_{rBC} and CO originate from similar combustion sources. A lower R^2 suggests that the two species may have different emission sources or that the sampled air masses were influenced by multiple plumes during transport. Russia covers a very large geographical area, and emissions differ substantially between its western and eastern regions. Such heterogeneity may reduce the correlation.

- Trajectory classification uncertainty: When we separate Russian air masses by altitude, the R^2 in the FT improves to 0.68, while it remains low (0.18) in the PBL. Air masses entering the Yellow Sea from Russia generally travel at higher altitudes; those sampled in the PBL are more likely to have interacted with plumes from Mongolia or China on route,

which can weaken the M_{rBC}–CO correlation.

These combined factors plausibly explain the lower R^2 for Russia compared with other source regions. We have added this discussion to the manuscript.

L 443–449:

"In addition, Russia-sourced air exhibited notable vertical contrasts in both tracer ratios and rBC-CO correlation. While the overall rBC-CO correlation was relatively weak (R^2 = 0.34; Figure 5), this likely reflects the heterogeneous emission sources across the vast Russian territory and the influence of mixed plumes during transport. However, when separated by altitude, the correlation improved significantly in the FT (R^2 = 0.68) but remained low in the PBL (R^2 = 0.18), suggesting greater mixing with other continental plumes at lower altitudes. This vertical pattern was further supported by lower rBC/CO and higher CO/CO_2 slopes in the PBL, likely influenced by additional CO emissions along the transport pathway, while the opposite was observed in the FT."

References:

Choi, Y., Kanaya, Y., Park, S. M., Matsuki, A., Sadanaga, Y., Kim, S. W., Uno, I., Pan, X., Lee, M., Kim, H., and Jung, D. H.: Regional variability in black carbon and carbon monoxide ratio from long-term observations over East Asia: assessment of representativeness for black carbon (BC) and carbon monoxide (CO) emission inventories, Atmos. Chem. Phys., 20, 83–98, https://doi.org/10.5194/acp-20-83-2020, 2020b.

Gu, J., Zhang, Y., Yang, N., and Wang, R.: Diurnal variability of the planetary boundary layer height estimated from radiosonde data, Earth Planet. Phys., 4, 479–492, https://doi.org/10.26464/epp2020042, 2020.

Hu, K., Zhao, D., Liu, D., Ding, S., Tian, P., Yu, C., Zhou, W., Huang, M., and Ding, D.: Estimating radiative impacts of black carbon associated with mixing state in the lower atmosphere over the northern North China Plain, Chemosphere, 252, 126455, https://doi.org/10.1016/j.chemosphere.2020.126455, 2020.

Hu, K., Liu, D., Tian, P., Wu, Y., Li, S., Zhao, D., Li, R., Sheng, J., Huang, M., Ding, D., Liu, Q., Jiang, X., Li, Q., and Tao, J.: Identifying the fraction of core–shell black carbon particles in a complex mixture to constrain the absorption enhancement by coatings, Environ. Sci. Technol. Lett., 9, 272–279, https://doi.org/10.1021/acs.estlett.2c00060, 2022.

Liu, D., Zhao, D., Xie, Z., Yu, C., Chen, Y., Tian, P., Ding, S., Hu, K., Lowe, D., Liu, Q., Zhou, W., Wang, F., Sheng, J., Kong, S., Hu, D., Wang, Z., Huang, M., and Ding, D.: Enhanced heating rate of black carbon above the planetary boundary layer over megacities in summertime, Environ. Res. Lett., 14, 124003, https://doi.org/10.1088/1748-9326/ab4872, 2019.

Qu, Y., Han, Y., Wu, Y., Gao, P., and Wang, T.: Study of PBLH and its correlation with particulate matter from one-year observation over Nanjing, Southeast China, Remote Sens., 9, 668, https://doi.org/10.3390/rs9070668, 2017.

Tian, P., Liu, D., Zhao, D., Yu, C., Liu, Q., Huang, M., Deng, Z., Ran, L., Wu, Y., Ding, S., Hu, K., Zhao, G., Zhao, C., and Ding, D.: In situ vertical characteristics of optical properties and heating rates of aerosol over Beijing, Atmos. Chem. Phys., 20, 2603–2622, https://doi.org/10.5194/acp-20-2603-2020, 2020.